

ON THE MEASUREMENT OF LOW-ENERGY SPUTTERING YIELD USING RUTHERFORD BACKSCATTERING SPECTROMETRY

V. SHUTTHANANDAN and Pradosh K. RAY
*College of Engineering, Architecture and Physical Sciences
Tuskegee University, Tuskegee, AL 36088*

N. R. SHIVAPARAN and Richard J. SMITH
*Physics Department
Montana State University, Bozeman, MT 59717*

S. THEVUTHASAN
*Environmental Molecular Sciences Laboratory
Pacific Northwest National Laboratory, Richland, WA 99352*

Maris A. MANTENIEKS
NASA-Lewis Research Center, Cleveland, OH 44135

Abstract

An experimental study is described to measure low-energy (less than 500 eV) sputtering yields of molybdenum with xenon ions using Rutherford backscattering spectrometry (RBS). An ion gun was used to generate the ion beam. The sputtered material was collected on a thin aluminum strip which was mounted on a semi-circular collector plate. The target was bombarded with 200 and 500 eV xenon ions at normal incidence. The differential sputtering yields were measured using the RBS method with 1 MeV helium ions. The differential yields were fitted with a cosine fitting function and integrated with respect to the solid angle to provide the total sputtering yields. The sputtering yields obtained using the RBS method are in reasonable agreement with those measured by other researchers using different techniques.

1. Introduction

NASA's Solar Electric Propulsion Technology Application Readiness (NASTAR) program has baselined the 30-cm xenon ion engine technology developed under the On-Board Propulsion (OBP) program. The NSTAR system is a prime candidate for application in early planetary missions being proposed to NASA's New Millennium initiative¹.

Flight qualification of an ion thruster requires a demonstrated life time of 5000 to 10000 hours or more. The principle life-limiting element in an ion propulsion system is the thruster ion optics².

Specifically, the two grid optics undergo two different sputtering processes. The accelerator grid biased negatively with respect to the discharge chamber, is subject to the impact of charge exchange ions produced just downstream of the grid³. They impinge on the downstream side of the grid with energies of approximately 200 eV. This effect is due to the higher than desired pressure in the test facilities. The positive grid is bombarded on the upstream side by low energy ions in the discharge chamber. The energy of these ions is approximately equal to the discharge voltage (25 V) for a 2.3-KW, 30-cm xenon thruster. It has been determined that practically all of the sputter erosion is due to the doubly charged ions peaked at the center of the thruster. The energy of the doubly charged ions is assumed to be twice the energy of the singly charged ions.

It has been observed that the energies of ions produced near a hollow cathode can be several times the anode-to-cathode potential difference⁴. The sputtered materials from these ion-surface interactions are deposited on to adjacent structures inside the discharge chamber. Subsequent formation of flakes when the sputtered materials of sufficient thickness peel off from these structures is also a major concern⁵⁻⁷.

Sputtering yields have been measured at low ion energies for various metal-ion combinations. However, there are uncertainties about the low-energy yield data, particularly below 200 eV. With a variety of surface conditions of the targets and the experimental techniques involved, it is not surprising that sputtering yield data reported by different authors show considerable variations. In view of this, we initiated an experimental investigation to measure sputtering yields at ion energies below 500 eV.

Four methods have been tried successfully to measure sputtering yields at low ion energies:

- (1) Weight loss method^{8,9}
- (2) Optical spectroscopy method¹⁰
- (3) Radioactive tracer method¹¹⁻¹³
- (4) Secondary neutral mass spectrometry^{14,15}

However, each method has its disadvantages. The weight loss method has been used extensively but this method requires a high ion current density to provide a measurable weight loss in a relatively short time. Hence, for low-energy measurements, sputtering was performed in plasma discharge systems. The optical spectroscopic method is also applicable in plasma discharge experiments. A general disadvantage of the plasma discharge systems is that the irradiation conditions are somewhat poorly defined and impurities in the plasma could contribute to the measured yields. Moreover, at ion energies near the sputtering threshold, different charge states of the ions could provide erroneous values of the sputtering yields.

The radioactive tracer method has been found to be highly sensitive, even near threshold energies. The disadvantage of the radioactive tracer method is that only a few suitable radioisotopes are available as tracers. For example, accelerator grids are made of molybdenum which do not have a suitable radioisotope. This prompted us to use a secondary neutral mass spectrometer (SNMS) as a detector of sputtered materials. However, SNMS spectra provide information on differential

sputtering yields only. Hence, these spectra have to be converted to total sputtering yields by some normalization process. Moreover, the angular distribution of the emitted particles changes slightly with energy at low incident ion energies, and for a mass spectrometer with a fixed angle-of-acceptance aperture, this introduces some error in sputtering yield measurements.

Sputtering yields can also be measured by depositing the sputtered material on a foil and subsequently measuring the amount of deposited materials by Rutherford backscattering spectrometry (RBS). The RBS technique can measure reliably as little as one monolayer of deposited material. The RBS method has been used in high-energy sputtering measurements¹⁶⁻¹⁸, but it has not been used in low-energy sputtering studies presumably due to the large amount of time required to deposit a measurable amount of sputtered material on the collector foil. We have initiated a systematic investigation of the applicability of the RBS technique in low-energy sputtering yield measurements. In this paper, we present the results of the first part of our study involving the sputtering of molybdenum with 200 and 500 eV xenon ions.

2. Theory

The RBS technique is a non-destructive surface analysis method where an energetic light ion beam is directed at the surface of the sample. The ions interact with atoms in the sample and some of them are backscattered into a detector. From the energy spectrum of backscattered ions one can infer considerable information about the sample's thickness and composition¹⁹.

A typical RBS spectrum from a thin film deposited on a single element substrate is shown in Fig. 1, where an ion beam with energy E_0 strikes the sample at normal incidence and backscattered ions are detected at a scattering angle θ . When thin films of high atomic numbers are deposited on a substrate of low atomic number, the peak and the continuum of the backscattered spectrum are well separated. The ions scattered from the surface atoms of the thin film will reach the detector with energy KE_0 ($K < 1$) where K is given by the following equation:

$$K = \frac{\left[\left(M_2^2 - M_1^2 \sin^2 \theta \right)^{1/2} + M_1 \cos \theta \right]^2}{M_1 + M_2} \quad (1)$$

Here, θ is the scattering angle, M_1 is the mass of the incident ion, and M_2 is the mass of the target atom.

The ions scattered from the atoms which are below the surface will give signals at energies less

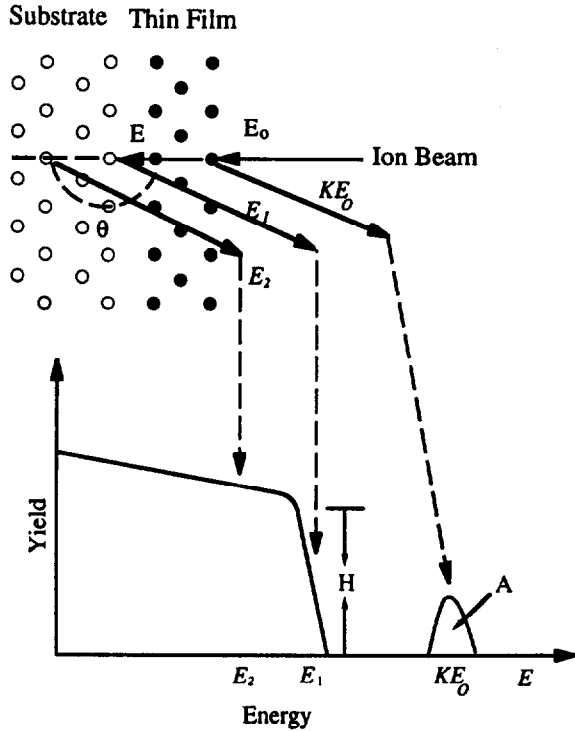


Fig. 1. Schematic diagram depicting the RBS technique.

than KE_0 , as shown in Fig. 1. The backscattered ion yield, A , from a thin film deposited on a light material substrate is given by,

$$A = QNt \left(\frac{d\sigma}{d\Omega} \right)_{film} \Omega \quad (2)$$

where, Q is the number of incident helium ions at the target, N is the atomic density (atoms/cm³), t is the thickness of the sputtered film, $d\sigma/d\Omega$ is the differential Rutherford scattering cross-section, and Ω is the solid angle subtended by the detector relative to the helium beam spot on the sample surface.

The backscattering yield in the surface region is equal to the area under the peak and this can be measured from the backscattered data. The parameter, $d\sigma/d\Omega$ is calculated from the following equation:

$$\frac{d\sigma}{d\Omega} = F \left(\frac{z_1 z_2 e^2}{2E_0 \sin^2 \theta} \right)^2 \frac{\left\{ 1 - \left(\frac{M_1 \sin \theta}{M_2} \right)^2 \right\}^{1/2} + \cos \theta}{\left[1 - \left(\frac{M_1 \sin \theta}{M_2} \right)^2 \right]^{1/2}} \quad (3)$$

where F is a screening correction factor and is given by

$$F = 1 - \frac{0.042 z_1 z_2^{4/3}}{E_0} \quad (4)$$

and E_0 is the energy of the incident helium ions in keV.

The backscattering yield from the surface of the substrate is proportional to the edge height, H , which is given by,

$$H = \frac{\Delta E}{[\varepsilon_0]} Q \left(\frac{d\sigma}{d\Omega} \right)_{Substrate} \Omega \quad (5)$$

where H is the edge height of the RBS spectrum, ΔE the width of a single channel of the spectrum, and $[\varepsilon_0]$ is given by the following equation:

$$[\varepsilon_0] = K\varepsilon(E_0) + \frac{\varepsilon(KE_0)}{\cos \theta} \quad (6)$$

where ε is the stopping cross section¹⁹.

From equations (2) and (5) the value of Nt is obtained as

$$Nt = \frac{A \Delta E}{H [\varepsilon_0]} \frac{\left(\frac{d\sigma}{d\Omega} \right)_{Substrate}}{\left(\frac{d\sigma}{d\Omega} \right)_{film}} \quad (7)$$

Thus the edge height (H) and the peak area (A) of the backscattered spectrum provide the Nt values.

We are interested in determining the differential sputtering yield $Y(\theta)$ which is defined as the number of sputtered atoms per incident ion per unit solid angle. Once the Nt values are obtained, $Y(\theta)$ can be calculated from the following equation:

$$Y(\theta) = \frac{R^2 Nt(\theta)q}{IT} \quad (8)$$

where R is the radius of the collector strip, q is 1.6×10^{-19} C/ion, I is the xenon beam current, and T is the total sputter time.

3. Experimental Procedure

The experiments were performed in a 22.5 cm diameter spherical chamber connected to a 170 l/s turbomolecular pump. A base pressure of 2×10^{-9} Torr was obtained after baking the chamber. A uniform ion beam current was maintained by a stabilized gas flow system. Xenon gas of 99.9995% purity was used in these studies. When xenon was introduced into the vacuum chamber, the pressure increased to 1×10^{-6} Torr.

It is well known that the presence of background gases has the effect of lowering the values of the measured sputtering yields. Nitrogen, for example, is easily chemisorbed on Mo and it will act as a buffer to the impinging ions, thus reducing the measured sputtering yields. To ensure that a dynamically clean sputtering condition exists, one can use the following criterion²⁰:

$$\frac{Y_{i,s} I}{f \beta_{i,s}} \geq 10 \quad (9)$$

where $Y_{i,s}$ is the sputtering yield of species i , I is the ion flux impinging on target s , f is the background gas flux impinging on target s , and $\beta_{i,s}$ is the sticking probability of background gas species on target s .

To calculate the ratio defined by Eq. (9), it is assumed that the bulk of the chemisorbed gas on the target surface is nitrogen. The sputtering yields of chemisorbed nitrogen were calculated using the formulation developed by Winters²⁰. At 200 eV, the sputtering yield of nitrogen for xenon ions is 0.2 atom/ion. The sticking coefficient is assumed to be equal to one because of the high reactivity of the species in the presence of the ion beam. For our experimental conditions, the ratio defined by Eq. (9) is estimated to be over 50 which is much higher than the recommended value of 10. Therefore, no reduction of the sputtering yield of Mo due to background gases is expected in our measurements.

The target was mounted on a XYZ θ manipulator for precise positioning within the vacuum chamber. During sputtering, the target was placed at a distance of 20 mm from the exit plane of the ion gun. At this position, the ion beam could be focused to a spot approximately 1 mm in diameter.

The target was bombarded by xenon ions at 200 and 500 eV at normal incidence, and the sputtered Mo atoms were collected on a thin, semi-circular collector foil as shown in Fig. 2. The foil was mounted on a 12.5 mm wide collector plate which formed a semi-circle of 15 mm radius around the position where the ion beam was focused on the target (Fig. 2). A 5 mm diameter hole in the center of the collector plate and the Al foil allowed the passage of the ion beam.

To determine if the surface condition of the target had any measurable effect on the sputtering yield, two different targets were used. Both targets were 12.5 mm in diameter and 6.2 mm in thickness and were cut from a rod of 99.5% purity. One of the targets was unpolished but cleaned with acetone and distilled water and the other target was electropolished.

All RBS measurements except one were performed at Montana State University (MSU). The sputter deposits from the electropolished sample were analyzed using the RBS facility at the Pacific Northwest National Laboratory (PNNL). In both cases, 1 MeV helium ions were used to probe the collector foil. The backscattered ions were detected by a solid-state detector located at 155° (MSU) and 165° (PNNL) to the direction of the helium ion beam. From the RBS data, the quantity Nt is determined as a function of ejection angle. The diameter of the He ion beam was 2 mm and hence the points where the measurements were made were 2 mm apart. Figure 3 shows the shape of the foil and points where the measurements were made.

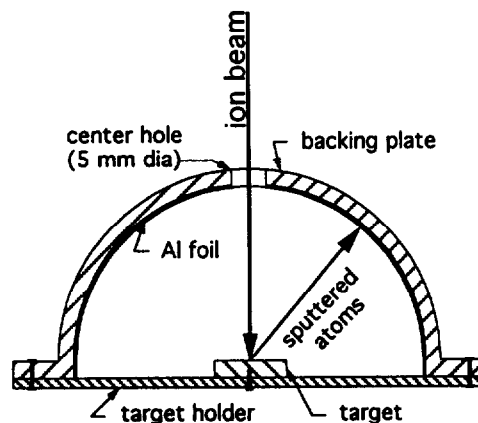


Fig. 2. Schematic diagram of the target-collector assembly.

In the case of high-energy sputtering (ion energies in the keV region), the sputtered atoms are observed to follow a cosine angular distribution. Thus, the function $A\cos^n\theta$ is generally used to fit the high-energy differential sputtering yield data. However, in low-energy sputtering, the angular distribution of the sputtered particles has been observed to be under-cosine. In order to retain the cosine character of the angular distribution, the differential sputtering yields obtained from Eq. (8) were fitted using the following function:

$$f(\theta) = A_1 \cos\theta + A_2 \cos^2\theta + A_3 \cos^3\theta + A_4 \cos^4\theta \quad (10)$$

The total sputtering yield is obtained by integrating $f(\theta)$ with respect to the solid angle:

$$Y_{tot} = \int f(\theta) 2\pi \sin\theta d\theta = 2\pi \left(\frac{A_1}{2} + \frac{A_2}{3} + \frac{A_3}{4} + \frac{A_4}{5} \right) \quad (11)$$

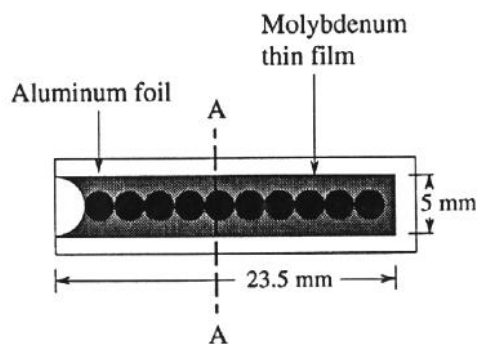


Fig. 3. Location of RBS measurements on the collector foil

4. Results and Discussion

One of the uncertainties in RBS measurements is the sticking coefficient of the sputtered particles on the substrate when the first monolayer is formed. Three different substrates were used in sputtering with 500 eV xenon ions to determine the substrate to which the sputtered particles adhere best. The substrates tested were plain aluminum foil (7 mil thick), plasma etched aluminum foil and grafoil. It was found that among the three substrates tested, the sticking probability of sputtered

Mo is highest on the plain aluminum foil and lowest on grafoil. Hence, all subsequent depositions were made on plain aluminum foils. In our RBS calculations, the sticking coefficient has been assumed to be one.

Sputter depositions from the unpolished target were made at both 200 and 500 eV whereas the electropolished target was sputtered only at 200 eV. All sputtering was done at normal incidence. For the 200 eV run, the plain target was bombarded for 50 hours while the electropolished target was sputtered for 34 hours. For the 500 eV run, the plain target was sputtered for 30 hours. The ion gun was run 8 to 10 hours each day to collect data.

To determine the uniformity of deposition across the width of each substrate, RBS measurements were first performed at around 45° target emission angle along line A-A (Fig. 3). The resulting Mo peak areas obtained from the unpolished sample are plotted in Fig. 4 for 200 and 500 eV incident ion energies. It can be seen from this figure that maximum Mo counts are obtained from the central portion of the collector foil. This region also happens to be larger than the helium beam diameter. The center of this region was determined in each run and along that line all subsequent RBS measurements were performed.

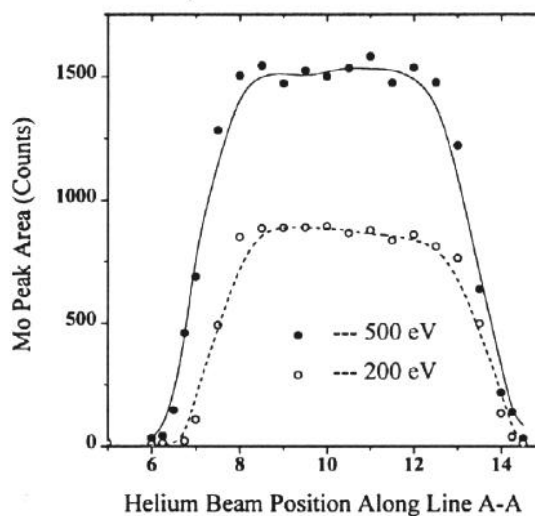


Fig. 4. Mo peak area as a function of He beam position across the foil at A-A.

The RBS measurements indicated that measurable amounts of sputtered material were deposited on all runs. The least amount of deposit was in excess of one monolayer at 82° target emission angle at 200 eV. Figure 5 shows a typical RBS spectrum taken at 200 eV at 44° target emission

angle. At this point, the thickness of the sputtered Mo was in excess of 6 monolayers. The Mo peak was well separated from the substrate backscattering continuum.

The polar plots of the differential sputtering yields obtained from RBS measurements from the unpolished target at 200 and 500 eV are presented in Fig. 6. It is apparent from this figure that the angular distributions of ejected particles are under-cosine. It is also observed that the maximum of this distribution shifts towards larger angles at lower incident ion energies. For example, at 500 eV the maximum occurs at around 45° whereas at 200 eV it is around 60° . The differential yields obtained for these two runs are also shown in Fig. 7 as a function of angle in Cartesian coordinates. They were fitted with the function described in Eq. (10) and integrated over all solid angles to provide total sputtering yields.

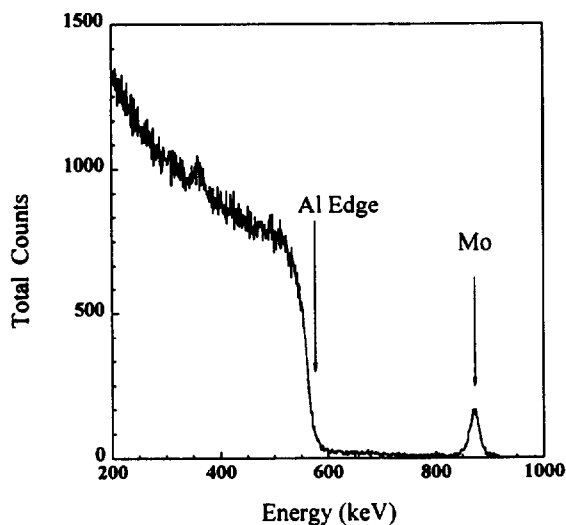


Fig. 5. A typical RBS spectrum from Mo deposited on Al foil.

The sputtering yields at 200 and 500 eV are presented in Fig. 8. In this figure, low-energy Mo sputtering data of Rosenberg and Wehner⁸ and of Weijnsfeld et al⁹ are also plotted for comparison. In both of these measurements, spherical targets were immersed in a low-pressure, high-density plasma and sputtering yields were determined from the weight loss of the target. The yields obtained by RBS measurements fall in the range of yields measured by these two groups of researchers. In a more recent experiment, thin films of molybdenum were sputtered by ions of xenon and other noble gases²¹. In the low-energy end, with xenon ions, sputtering

yields were found to be 0.8 at 200 eV and 1.6 at 500 eV. Since, these values are considerably higher than those obtained by other researchers, these values are not shown in Fig. 8.

The sputtering yields measured by Rosenberg and Wehner are found to be consistently higher (17% at 600 eV and 62.5% at 100 eV) than those obtained by Weijnsfeld et al. The yield measured by the RBS method at 500 eV agrees with Weijnsfeld's data but at 200 eV they are lower by 27% for the unpolished sample and 14% for the electropolished sample. The fact that the electropolished sample provides a slightly higher yield compared to the unpolished sample indicates that in sputtering yield measurements surface preparation plays some role.

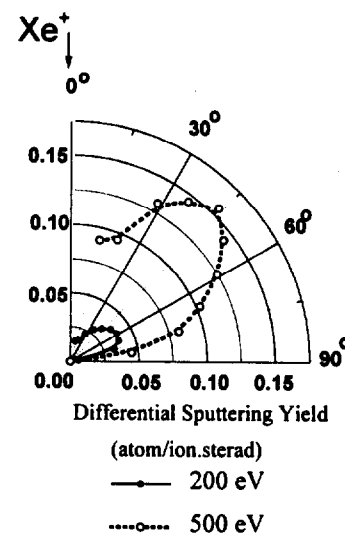


Fig. 6. Polar plot of the differential sputtering yield of Mo at 200 and 500 eV.

Two factors may influence the sputtering yield measurements using the RBS method. The first one is the sticking coefficient. In this calculation, the sticking coefficient of sputtered Mo atom on the Al foil has been taken as one. However, the sticking coefficient may be less than one when the first monolayer is being formed. Since, the measurement involves only a few monolayers at the most, this introduces some error in the calculation and the actual sputtering yields should be somewhat higher than what is reported here.

The other factor is the assumption that the angular distribution of the sputtered particles is

isotropic. This assumption may not be quite accurate. Polycrystalline metal targets have preferred orientation and atoms sputtered from several targets have been observed to be preferentially ejected in the closed-packed direction²². If this is true for Mo, the integration of the measured differential sputtering yields over all solid angles would introduce some error.

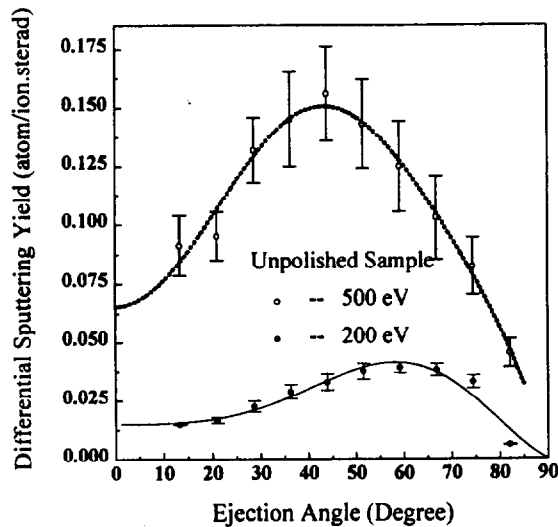


Fig. 7. Differential sputtering yield of Mo in Cartesian coordinates at 200 and 500 eV.

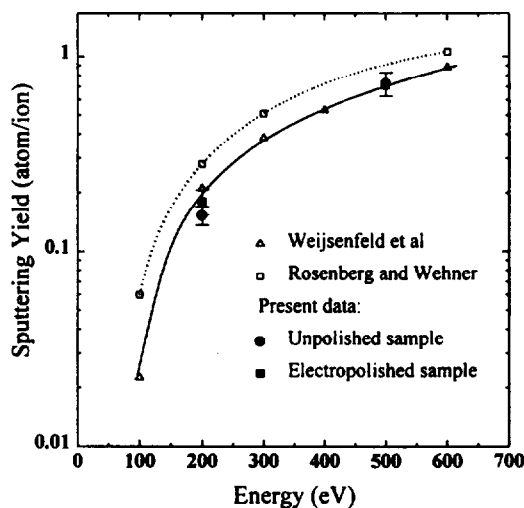


Fig. 8. Total sputtering yield of Mo at 200 and 500 eV.

5. Conclusions

Sputtering yields of Mo by xenon ions at 200 eV and 500 eV at normal incidence have been measured using the RBS method. An ion gun was used to produce xenon ions. The values of sputtering yields obtained in this manner are in the range of those measured by other researchers using different techniques. Thus, the RBS method can be successfully used in low-energy sputtering measurements.

Two issues need to be addressed in any future work in low-energy sputtering yield measurements using the RBS method. One is the sticking coefficient of sputtered atoms on the substrate as the first monolayer is formed. The other is the assumption of isotropic angular emission of sputtered particles in the hemispherical space where these particles are ejected.

6. Acknowledgments

This research was supported through NASA research grants NAG3-1388 and NAG3-2037. The work at Montana State University was supported through NASA EPSCoR Grant NCCW-0058.

7. References

1. F. M. Curran and L. W. Callahan, "The NASA On-Board propulsion program" AIAA-95-2379 (1995).
2. M. J. Patterson, "Low- I_{sp} derated thruster operation," AIAA-92-3203 (1992).
3. X. Peng, D. Keefer, and W. M. Ruyten, "Plasma particle simulation of electrostatic ion thrusters," *Journal of Propulsion and Power*, **8**, 361 (1992).
4. V. J. Friedly, "Hollow cathode operation at high discharge currents," NASA CR-185238 (1990).
5. J. R. Beattie and J. N. Matossian, "Mercury ion thruster technology," NASA CR 174974 (1989).
6. Patterson, V. K. Rawlin, J. S. Sovey, M. J. Kussmaul and J. Parks, "2.3 kW ion thruster wear test," AIAA-95-2516 (1995).
7. K. Rawlin, "Internal erosion rates of a 10-kW xenon ion thruster," Paper No. AIAA-88-2912 (1988).
8. Rosenberg and G. K. Wehner, "Sputtering yields for low-energy He⁺, Kr⁺, and Xe⁺ ion bombardment," *J. Appl. Phys.* **33**, 1842 (1962).
9. C. H. Weijnsfeld, A. Hoogendoorn, and M. Koedam, "Sputtering of polycrystalline metals

- by inert gas ions of low-energy (100-1000 eV)", *Physica* **27**, 763 (1961).
10. R. V. Stuart and G. K. Wehner, "Sputtering yields at very low bombarding ion energies", *J. Appl. Phys.* **33**, 2345 (1962).
 11. N. D. Morgulis and V. D. Tischenko, "The investigation of cathode sputtering in the near threshold region," *Soviet Phys.-JETP* **3**, 52 (1956).
 12. A. K. Handoo and P. K. Ray, "Sputtering yield of chromium by argon and xenon ions with energies from 50 to 500 eV," *Appl. Phys.* **A54**, 92 (1992).
 13. A. K. Handoo and P. K. Ray, "Sputtering of cobalt and chromium by argon and xenon ions near threshold energy region," *Can. J. Phys.* **71**, 155 (1993).
 14. H. Oechsner, H. Schoof and E. Stumpe, "Sputtering of Ta₂O₅ by Ar⁺ ions at energies below 1 keV", *Surf. Sci.* **76**, 343 (1978).
 15. S. Bhattacharjee, J. Zhang, V. Shutthanandan, and P.K. Ray, "Application of secondary neutral mass spectrometry in low-energy sputtering yield measurements" *Nucl. Instr. Meth. Phys. Res. B* **129**, 123 (1997).
 16. G. Kiriakidis, C. E. Christodoulides, G. Carter and J. S. Colligon, "An RBS technique for measurement of the erosion of ion implanted films," *Appl. Phys.* **19**, 191 (1979).
 17. H. L. Bay, J. Bohdansky, W. O. Hofer and J. Roth, "Angular distribution and differential yields for low-energy light-ion irradiation of polycrystalline nickel and tungsten" *Appl. Phys.* **21**, 327 (1980).
 18. N. P. Tognetti, R. P. Webb, C. E. Christodoulides, D. G. Armour and G. Carter, "Ion bombardment induced interface mixing in the Ag-Si system," *Nucl. Instr. Meth.* **182/183**, 107 (1981).
 19. L. C. Feldman and J. W. Mayer, *Fundamentals of Surface and Thin Film Analysis*, North-Holland, New York (1986).
 20. H. F. Winters and E. Taglauer, "Sputtering of chemisorbed nitrogen from single crystal planes of tungsten and molybdenum", *Phys. Rev. B* **35**, 2174 (1987).
 21. P. C. Zalm, "Energy dependence of the sputtering yield of silicon bombarded with neon, argon, krypton and xenon ions," *J. Appl. Phys.* **54**, 2660 (1983).
 22. H. Tsuge and S. Esho, "Angular distribution of sputtered atoms from polycrystalline metal targets" *J. Appl. Phys.* **52**, 4391 (1981).